Published in final edited form as:
Toxicology. 2012 December 16; 302(2-3): 114–122. doi:10.1016/j.tox.2012.09.008.

Multi-Walled Carbon Nanotube Directed Gene and Protein Expression in Cultured Human Aortic Endothelial Cells is Influenced by Suspension Medium

Achini K. Vidanapathirana[a], **Xianyin Lai**[b], **Susana C. Hilderbrand**[c], **Josh E. Pitzer**[c], **Ramakrishna Podila**[c], **Susan J. Sumner**[d], **Timothy R. Fennell**[d], **Christopher J. Wingard**[a], **Frank A. Witzmann**[b], and **Jared M. Brown**[c]

[a]Department of Physiology, Brody School of Medicine, East Carolina University, Greenville, NC, USA

[b]Department of Cellular and Integrative Physiology, Indiana University School of Medicine, Indianapolis, IN, USA

[c]Department of Pharmacology & Toxicology, Brody School of Medicine, East Carolina University, Greenville, NC, USA

[d]RTI International, RTP, NC, USA

Abstract

The use and production of multi-walled carbon nanotubes (MWCNTs) have significantly increased over the last decade due to their versatility in numerous applications. Their unique physical and chemical properties make them desirable for various biomedical applications, but the same properties also raise concerns about their safety to human health, particularly at the cellular level. The vascular endothelium could be exposed to nanomaterials either by direct intravenous administration in nanomedicine or by translocation following inhalational exposure in an occupational setting. We hypothesized that direct exposure to MWCNTs will increase the expression of inflammatory markers in human aortic endothelial cells (HAEC). We also investigated the effect of the route of exposure on activation by changing the suspension medium of the MWCNTs. HAEC were treated *in vitro* with MWCNTs (1 or 10 μg/cm^2) suspended in either cell culture medium [(M)-MWCNTs] or 10% clinical grade pulmonary surfactant [(S)-MWCNTs]. The zeta potential of the (S)-MWCNTs was significantly more negative than the (M)-MWCNTs suggesting a more stable suspension. Treatment of HAEC with (S)-MWCNTs; as compared to (M)-MWCNTs resulted in a significantly higher up-regulation of mRNA transcripts for cell adhesion molecules *VCAM1, SELE, ICAM1* and the chemokine *CCL2*. Time dependent changes in VCAM1 and CCL2 protein levels were confirmed by immunofluorescence, flow cytometry and ELISA. A label free quantitative mass spectrometry proteomic analysis was utilized to compare protein expression patterns between the two suspensions of MWCNTs. We identified significant expression changes in >200 unique proteins in MWCNT treated HAEC. However, the

Corresponding author: Jared M. Brown, Ph.D., Department of Pharmacology and Toxicology, Brody School of Medicine, East Carolina University, Brody Medical Sciences Building, Rm 6W35, 600 Moye Boulevard, Greenville, NC 27834, USA, brownja@ecu.edu, Tel. office- 252-744-2108, Fax: 252-744-3203.

Conflicts of interests

The authors declare that they have no conflicts of interests.

two suspensions of MWCNTs resulted in different protein expression patterns with the eIF2 pathway as the only common pathway identified between the two suspensions. These data suggest that direct exposure to MWCNTs induces acute inflammatory and protein expression changes in HAEC, which is influenced by the type of media used for suspension of MWCNTs and their resulting zeta potential.

Keywords

MWCNT; surfactant; eIF2; nanotoxicology; nanomedicine; protein corona

1. Introduction

With advancement of nanotechnology, novel carbon nanomaterials are being engineered and thereby expanding their use in various industries. Biomedical applications of nanomaterials are equally advancing with the use of nanocatalysts, dendrimers and nanosensors for both therapeutic and diagnostic applications. Following functionalization, carbon nanotubes are useful as tracers of sentinel lymph nodes (Li et al., 2010) vascular grafts designs, antigen (Bianco et al., 2005) and drug delivery tools by both passive and active targeting (Sinha et al., 2006). The unique physicochemical properties of the multi-walled carbon nanotubes (MWCNTs) such as high electrical conductivity, large surface area to mass ratio, strength and functionalization potential make them versatile in many applications (Dai, 2002). These emerging trends in nanotechnology increase the environmental and occupational exposure to nanomaterials via inhalation and therapeutic exposure via intravenous administration, resulting in potential health risks to various populations. In order to use nanomaterials as a successful vehicle for drug, gene or antigen delivery, they should be compatible with the internal biological environment and act as inert substances. As with any drug, the demarcation between therapeutic and toxic doses for nanoparticles and identification of the factors that potentiate toxicity is crucial in determining their pharmacological relevance. Sufficient information is not currently available on these factors and mechanisms of toxicity for MWCNTs.

Due to their small size, nanomaterials merit attention for their effects on the cardiovascular system due to potential increases in their penetrability to different tissues and to sub-cellular locations. Engineered nanoparticles can enter the systemic circulation through different routes. The main pathway that has been studied is pulmonary exposure and subsequent translocation out of the lung. This route of exposure is generally thought to result in relatively low concentrations of nanoparticles in the systemic circulation in contrast to those following intravenous administration (Kim et al., 2010; Li et al., 2007; van der Zande et al., 2011). In addition, nanoparticles are also known to translocate immediately to the lymphatic system as early as six hours following inhalational exposure (Aiso et al., 2011). Using intravenous nanomaterials for diagnostics or drug delivery could lead to higher concentrations in blood (Lacerda et al., 2008; Wenger et al., 2011). Nanoparticle exposure via any of these routes imposes a risk to the vascular endothelium that serves as a critical interface between blood and tissue. Any disruption in endothelial function or alteration in permeability can account for alterations in the overall functioning of the associated organ or tissue.

There is increasing evidence for effects of the ‘protein corona’ that is associated with nanoparticles when they are applied to *in vitro* and *in vivo* systems. The serum proteins that adhere to the surface of nanoparticles and form the protein corona affect the transport and metabolism of nanoparticles (Lundqvist et al., 2011). The dispersal state and associated functionalization of MWCNTs are known to correlate with intracellular distribution and pro-fibrotic changes of the murine lung (Wang et al., 2011b). Considering this evidence, the medium used for suspension becomes critical in designing nanomaterials for intravenous drug delivery.

We hypothesized that *in vitro* exposure of Human Aortic Endothelial Cells (HAEC) to MWCNTs results in increased expression of inflammatory markers that is dependent upon the suspension media used to disperse the MWCNTs. We initially focused on a limited number of cell adhesion molecules and inflammatory cytokines associated with endothelial cell activation and extended it to a proteomic analysis. As will be shown, the type of media used to suspend MWCNTs has significant influence on endothelial cell responses to MWCNT exposure that is likely due to changes in MWCNT agglomeration size and zeta potential.

2. Material and Methods

2.1. MWCNT suspension and characterization

Multi-walled carbon nanotubes (MWCNTs) were a generous gift from NanoTechLabs Inc. (Yadkinville, NC, USA). The dry powder form of the MWCNTs were previously characterized (Wang et al., 2011a) by transmission and scanning electron microscopy to obtain length, diameter distribution and elemental composition; Raman spectra; and the surface area, pore volume and pore size distribution of the MWCNTs were obtained based on the Brunauer-Emmett-Teller (BET) equation (Brunauer, 1938) and the Barrett-Joyner-Halenda (BJH) method (Barrett, 1951). The MWCNTs were suspended in 1 mg/ml suspensions in either 10% clinical grade surfactant (Infasurf®, ONY, Inc., Amherst, NY, USA) in saline [(S)-MWCNTs] or in culture medium [(M)-MWCNTs] and the mixture was cup-horn sonicated for 4 min using a Misonix ultrasonic liquid processor -1510R-MTH (Branson Ultrasonics Corp. Danbury, CT, USA). The hydrodynamic size distribution, a parameter describing the effective diameter of a diffusing particle, was characterized using dynamic light scattering (Nanosizer S90, Malvern Instruments, UK). The zeta potential, the primary indicator for describing the surface charge and stability of MWCNT suspension, was determined using a zeta potential device (Zeta ZS, Malvern Instruments, UK).

2.2. Cell culture

Human aortic endothelial cells (HAEC) were purchased from Cascade Biologics (Eugene, OR, USA) and cultured as recommended by the manufacturer, in Medium 200 with low serum growth supplement (LSGS, Life Technologies, Carlsbad, CA, USA) and antibiotics (Primocin 50 μg/1000ml, InvivoGen, SanDiego, CA, USA). The culture was maintained at 37°C in 5% humidified CO_2. Culture medium was changed every 48 h until reaching >80% confluence, then subsequently changed every 24 h. Cells were detached using 0.025% Trypsin with 0.01% EDTA and Trypsin neutralizer solution; PBS containing 0.5% newborn bovine serum (Life Technologies, Carlsbad, CA, USA) to obtain subcultures for MWCNT treatment. Cell viability was assessed 2, 6 and 24 h after treatment with (M)-MWCNTs or (S)-MWCNTs using two different assays (MTS assay and a live/dead cell assay). Since both assays did not reveal significant changes in cell viability following MWCNT exposure, these cells were used for further gene and protein expression analysis.

2.3. Exposure of HAEC to MWCNTs

Confluent HAEC (>90%) in passages 3–6 were used for this study. Each six well plate was seeded with 300,000 – 400,000 cells/well and treated with two doses; 1 and 10 μg/cm^2 of (M)-MWCNTs or (S)-MWCNTs. Untreated cells and cells treated with equal volumes of 10% surfactant were used as the controls. The total volume of fluid each well in a six well plate during the exposure in was 1 ml and the approximate height of the fluid column was

0.1 cm. The final concentration of the surfactant in the cell culture medium following treatment was 0.95%.

2.4. Cell Viability

CellTiter 96 Aqueous One Solution Cell Proliferation Assay (Promega, CA, USA) was used to assess cell viability following 2, 6 and 24 h of treatment with (M)-MWCNTs or (S)-MWCNTs. Cell culture supernatant was removed and 100 μl of phenol red free Dulbecco's Modified Eagle's Medium (DMEM) with 20 μl of the MTS (3-(4,5-dimethylthiazol-2-yl)-5-(3-carboxymethoxyphenyl)-2-(4-sulfophenyl)-2H-tetrazolium) reagent was added to each cell. The cells were incubated at 37°C in 5% humidified CO_2 for 30 min. A Synergy HT (Biotek VT, USA) plate reader was used to measure the absorbance at 490 nm. Cellular viability was calculated using the equation: % cellular viability = 100 × (*test sample absorbance/control absorbance*). In addition, HAECs following 24 h of exposure to (M)-MWCNTs or (S)-MWCNTs were assessed for cell viability using the Live/Dead Viability/Cytotoxicity Kit for mammalian cells (Molecular Probes, Invitrogen detection technologies, OR, USA). Samples were stained with Calcein AM and Ethidium homodimer under the manufacturer's instructions and flow cytometric analysis was done for 10000 cell events using an Accuri C6 flow cytometer (BD Accuri Cytometers Ann Arbor, MI, USA).

2.5. Real time-PCR

Total RNA isolated from HAEC was collected using Trizol reagent and chloroform degradation 2 h following exposure to MWCNTs. mRNA was quantified using a Nanodrop 2000 spectrophotometer (Thermo Scientific, USA) and reverse transcribed to cDNA using the Quanti-Tect reverse transcription kit (Qiagen, USA). We measured the expression of *VCAM1, CCL2, ICAM1, SELE,* and *IL8* by quantitative real time PCR using Quantitect primer assays and SYBR green master mix (Qiagen, USA). The cycle threshold (Ct) values for the targets and the internal reference were obtained using an Applied Biosystems StepOnePlus Real-Time PCR system (ABI, Carlsbad, CA, USA). In our preliminary experiments the expression of five housekeeping genes (*B2M, HPRT1, RPL13A, GAPDH* and *ACTB*) following MWCNT treatment was assessed using a PCR array. Since there were no significant difference in the level of mRNA expression across housekeeping genes, target cDNA levels were normalized to the internal reference: *GAPDH*, using the ΔΔCt method. Three or four independent experiments were used to determine the average fold changes for each target gene.

2.6. Flow cytometric analysis

HAEC treated with 10 $\mu g/cm^2$ of (M)-MWCNTs or (S)-MWCNTs for 2, 6 and 24 h were detached using 0.025% Trypsin ETDA (Life Technologies, Carlsbad, CA, USA) and resuspended in flow cytometry staining buffer (eBioscience, CA, USA). 10 ng/ml of recombinant human TNF α (PeproTech, NJ, USA) was used as a positive control (Schmidt et al., 2002). The anti-human SELE (ELAM1, CD62E) conjugated with fluorescein isothiocyanate (FITC) and anti-human VCAM1 (CD106) conjugated with phycoerythrin (PE, eBioscience, CA, USA) antibodies were diluted 1:500 in the staining buffer and incubated for 30 min at room temperature in the dark. After incubation the cells were washed and resuspended in staining buffer. Flow cytometric analysis was done for 10000 events using an Accuri C6 flow cytometer (BD Accuri Cytometers Ann Arbor, MI USA). Data and image analysis was performed with FCS Express 4 software (De Novo Software, Los Angeles, CA, USA).

2.7. ELISA

The supernatant of HAEC cultures was collected following 2, 6, and 24 h of exposure to MWCNTs suspended in either (M)-MWCNTs or (S)-MWCNTs. A Duoset ELISA (R & D Systems, MN, USA) was used according to the manufacturer's instructions to quantify human CCL2/ MCP1 levels in the supernatant. A Synergy HT (Biotek VT, USA) plate reader was used at 495 nm to detect CCL2 levels based upon a standard curve.

2.8. Immunofluorescence imaging

HAEC were grown on coverslips and treated with 1 and 10 μg/cm^2 of (M)-MWCNTs or (S)-MWCNTs for 6 h at >90% confluence. HAEC treated with 10 ng/ml of recombinant human TNF α (PeproTech, NJ, USA) for 6 h was used as a positive control. Following treatment cells were washed with phosphate buffered saline (PBS) with 0.2% Tween. Tris buffered saline (TBS), 0.2% Tween and 1% bovine serum albumin were used for blocking. The anti-human SELE (ELAM1, CD62E) conjugated with fluorescein isothiocyanate (FITC) and anti-human VCAM1 (CD106) conjugated with phycoerythrin (PE, eBioscience, CA, USA) antibodies were used for staining at 1:200 dilution. Prolong Gold Antifade reagent with DAPI (4′, 6-diamidino-2-phenylindole, Molecular Probes, NY, USA) was used to localize the nucleus. Immunofluorescence imaging was performed under 40X objective on an Olympus BX41 microscope and Olympus DP71 camera (Olympus America Inc. PA, USA).

2.9. Proteomics and Pathway analysis

HAEC treated with 1 and 10 μg/cm^2 of (M)-MWCNTs or (S)-MWCNTs for 24 h were washed with isotonic sucrose and frozen until further analysis. Adherent cells were solubilized by adding 500 μl of lysis buffer (8 M urea and 10 mM dithiothreitol, DTT) to each well. Cells were incubated at 35°C for 1 h with agitation, transferred to an ultracentrifuge tube, briefly vortexed, and centrifuged at 100,000 × g for 20 min at 4°C to pellet insoluble materials. The fully solubilized cell protein supernatant samples were then stored at −80°C until analysis. Protein concentration was determined by the Bradford Protein Assay (Bio-Rad, Hercules, CA, USA). A 60 μg aliquot of each sample was adjusted to a 262.5 μl volume with 8 M urea and 200 μl of a reduction/alkylation cocktail containing triethylphosphine and iodoethanol were added, as described (Lai et al., 2008). After incubation for 1 h at 35 °C, the reaction mixture was Speedvacced for 5 h to total dryness. A 100 μl volume of a 100 mM NH_4HCO_3 solution and 250 μl of H_2O were added to the dried sample tube and vortexed to dissolve the dried pellets completely. A 150 μl aliquot of a 20 μg/ml trypsin solution was added to each sample and incubated at 35°C for 3 h. Following 3 h of incubation another 150 μl of trypsin was added, and the solution incubated at 35°C for 3 h resulting in a final urea concentration of 3.2 M (n=5; 5 samples for each dose). HAEC proteins in each sample were then identified and quantified as technical replicates using a label-free quantitative mass spectrometry (LFQMS) approach as described (Lai et al., 2011).

Comparison of the abundance of individual protein dose-group means generated by LFQMS was performed within the IdentiQuantXL™ platform using one-way ANOVA and *post hoc* Pairwise Multiple Comparisons (Holm-Sidak method). Critical F-ratio significance for ANOVA was set at $p < 0.01$ and pairwise comparison at $p < 0.05$. False Discovery Rate (FDR) (Storey, 2002) was estimated using Q-value software. To interpret the biological relevance of the differential protein expression data and to compare biological effects across different MWCNT suspensions and exposure levels, protein lists and their corresponding expression values (fold change) were uploaded onto the Ingenuity Pathway Analysis (IPA) software server (http://www.ingenuity.com) and analyzed using the Core Analysis module to rank the proteins into top molecular and cellular functions and canonical pathways. The IPA Functional Analysis identified the biological functions that were most significantly related to the protein data set. Differentially expressed proteins from the dataset that were associated with biological functions in Ingenuity's Knowledge Base were considered for the analysis. Right-tailed Fisher's exact test was used to calculate a *p*-value determining the probability that each biological function assigned to that data set is due to chance alone. The Canonical Pathways Analysis identified the pathways from IPA's library of canonical pathways that were most significantly related to the data set. As above, differentially expressed proteins from the dataset that were associated with a canonical pathway in Ingenuity's Knowledge Base were considered for the analysis. The significance of the association between the protein data set and the canonical pathway was measured in 2 ways: 1) A ratio of the number of molecules from the data set that map to the pathway divided by the total number of molecules that map to the canonical pathway is displayed. 2) Fisher's exact test was used to calculate a p-value determining the probability that the association between the genes in the dataset and the canonical pathway is explained by chance alone. Submitted proteins were that were "Network Eligible" molecules and their fold changes were overlaid onto a global molecular network developed from information contained in Ingenuity's Knowledge Base. Functional networks were then algorithmically generated based on their connectivity.

2.10. Statistical Analysis

GraphPad Prism 5 software (GraphPad, SanDiego, CA, USA) was used for statistical analysis. Data are presented as means ± SEM and differences were considered statistically significant if $p < 0.05$. One-way ANOVA and post hoc Pairwise Multiple Comparisons (Holm-Sidak method) were used in the proteomics analysis. A one tailed t test was done to compare mRNA expression levels between different treatment groups.

3. Results

3.1. MWCNT suspension and characterization

Characterization details of the dry powder form of the MWCNTs used in this study have been published earlier (Wang et al., 2011a) and are summarized in Table 1. MWCNTs were suspended in either HAEC cell culture medium [(M)-MWCNT] or 10% pulmonary surfactant in saline [(S)-MWCNT] and hydrodynamic size and zeta potential were determined for the two suspensions. The zeta potential was remarkably different between the two suspensions of MWCNTs (Table 2) suggesting differences in stability of the suspension. The use of surfactant as a suspension medium provided better MWCNT stability based upon the zeta potential (−57 mV) versus a zeta potential of −15 mV in the (M)-MWCNT suspension. The use of (S)-MWCNTs also simulates the MWCNTs reaching the systemic circulation by its initial suspension in the lung surfactant as may occur with inhalational exposure.

3.2. Cell viability following MWCNT treatment

HAEC exposure to 1 and 10 $\mu g/cm^2$ MWCNTs in both types of suspensions for up to 24 h did not result in cytotoxicity (Table 3). Treated and untreated cells showed a mean cell viability of more than 87.7 %, as assessed by the MTS assay and the mean dead cells were less than 5.6% as determined by the Live/Dead cell assay.

3.3. Changes in gene expression of MWCNT treated HAEC

To determine effects of MWCNTs on HAEC, expression of key inflammatory markers related to endothelial cell biology was examined 2 h following treatment of HAEC with 1 and 10 $\mu g/cm^2$ MWCNTs. The expression of mRNA for *VCAM, SELE, IL8* and *CCL2* was up regulated with exposure to 10 $\mu g/cm^2$ (S)-MWCNTs but not (M)-MWCNTs (Figure 1). The ΔCt values did not significantly vary between the two vehicle controls for any gene studied except for CCL2 (supplementary data table 1). *CCL2 and SELE* were significantly increased, while *VCAM1* displayed a mean 75-fold increase with (S)-MWCNT treatment but did not reach statistical significance. In contrast, an increase in mRNA of these genes was not found with either of the two doses of (M)-MWCNTs.

3.4. Expression of cell adhesion molecules following MWCNT treatment of HAEC

Based on mRNA expression patterns, we performed flow cytometric analysis for VCAM1 and SELE at 2, 6 and 24 h following treatment with 10 μg/cm^2 of (M)-MWCNTs or (S)-MWCNTs. Representative histograms are shown for each time point in Figure 2. A minimal increase in VCAM1 was observed over time with MWCNT treatment (Figure 2). Similar changes were not evident with SELE at any time point with either suspension (data not shown). Surface protein expression of VCAM1 and SELE was confirmed by immunofluorescence imaging of HAEC grown on coverslips to avoid trypsinization effects. Similar to results obtained by flow cytometry, a minimal increase in VCAM1 and SELE following exposure to 10 μg/cm^2 of (S)-MWCNTs was observed (Figure 3). Changes in VCAM1 and SELE expression were not seen at 1 μg/cm^2 with either of the MWCNT suspensions.

3.5. HAEC production of CCL2 following MWCNT treatment

CCL2 protein levels were examined in the supernatant of HAEC treated 10 μg/cm^2 of (M)-MWCNTs or (S)-MWCNTs. Significant changes were seen at 6 and 24 h following treatment of HAEC with 10 μg/cm^2 of (S)-MWCNTs (Figure 4). In contrast, but consistent with mRNA expression, treatment of HAEC with (M)-MWCNTs did not induce significant differences in CCL2 levels.

3.6. Proteomics and pathway analysis

A LFQMS approach was used to analyze the expression of different proteins in HAEC treated with (M)-MWCNTs or (S)-MWCNTs. The approach resulted in the identification of 8,029 peptides leading to 6,684 statistically significant protein database hits. These hits represented 2,959 unique proteins that were qualified for quantitation and their abundance compared. Statistically significant changes were seen in specific protein levels 24 h following treatment with both doses (1 and 10 μg/cm^2) and both suspensions (Supplementary Table 2). The proteins that had significant fold changes were different and unique for each dose of MWCNT in each suspension. A dose related up-regulation was identified in only a few proteins. A summary of the number of proteins identified in each category and the overlap between the two doses are shown in Figure 5. The pathway analysis identified different pathways that significantly varied in activation among the two doses and the two MWCNT suspensions. The activation of eukaryotic activation factor 2 (eIF2) signaling pathway was the only common pathway identified with both doses and both types of MWCNT suspensions (Figure 6 A, B and supplementary Table 3). Pathway analysis was also used to identify different cellular mechanisms that changed with each dose of MWCNTs (Figure 6 C and D and supplementary Table 4).

4. Discussion

In this study, we found a moderate, but significant increase in the expression of different inflammatory genes and proteins along with an activation of different intracellular pathways in HAEC following direct exposure to MWCNTs that was dependent on the suspension of MWCNTs. These changes included an increase in the expression of chemokines and cell adhesion molecules with exposure to MWCNTs. In general, we observed greater cell responses with (S)-MWCNTs suggesting that the biomolecules attached to MWCNTs, as well as their zeta potential, play an important role in activation of intracellular pathways.

Analysis of proteomic data revealed the eukaryotic Initiation Factor 2 (eIF2) signaling pathway, which is often up-regulated in response to environmental stress and can suppress global protein translation, as the only common pathway activated when comparing across doses and suspensions of MWCNTs.

In this study, we compared the effects of two different MWCNT suspensions to simulate and speculate on effects of two different routes of exposure. Suspension of MWCNTs in cell culture medium was utilized to simulate a direct exposure to the endothelium as might be experienced following intravenous administration of nanotubes for diagnostic or therapeutic purposes. On the other hand, during an inhalational exposure, MWCNTs will encounter the surfactant lining of the alveolar epithelium before they are translocated to the systemic circulation across the alveolar capillary membrane. Therefore, we suspended MWCNTs in 10% surfactant prior to adding them to HAEC cultures. Lastly, the *in vitro* approach that we used allowed studying the direct, independent impact of the MWCNTs on endothelial cells without the confounding influence of inflammatory cells and/or autonomic nervous system activation associated with inhalational exposure on potential cardiovascular system changes.

A recent study using MWCNTs in pulmonary surfactant and serum suspensions in a cell free medium identified markedly varying patterns of adsorption of biomolecules to the nanotubes (Gasser et al., 2010). The implications of this difference were also demonstrated in our findings in an *in vitro* model. Considering the size of the nanoparticles and previous evidence on translocation (Aiso et al., 2011), it is reasonable to assume that the phospholipid and protein coating that forms on the MWCNTs can also be translocated along with the nanotubes across the alveolar capillary membrane to the circulatory system. These particles loaded with scavenger proteins can potentially reach cellular and sub-cellular locations of the endothelium in different tissues and alter the intracellular signaling pathways. The difference in zeta potential seen in our characterization data is indicative of the difference in dispersion and stability of MWCNTs in the two different media that results from formation of a protein corona. Even though the hydrodynamic sizes of the MWCNTs in suspensions are similar initially, they agglomerate at different rates which are indicted by the changes in the zeta potential. This is further supported by the difference in cellular responses to MWCNTs of the two suspensions. According to our data, the presence of (S)-MWCNTs initiates a greater inflammatory response when compared with the (M)-MWCNTs, which is augmented by increasing the dose of MWCNTs. This apparent increase in cell activation by (S)-MWCNTs suggests that the more negative zeta potential of the MWCNTs significantly contributes to toxicity. However, future studies should address the protein or lipid components that form the MWCNT corona in the suspensions used in this study and how they influence these responses. Interestingly, a recent study also reported on how the dispersal state of MWCNTs determined by the purity and suspension medium effected both *in vitro* and *in vivo* pro-fibrotic changes and intracellular localization of MWCNTs in lung epithelial cells (Wang et al., 2011b). Overall, this observation in our *in vitro* system suggests that the medium used for nanoparticle delivery and hence the route of exposure may have a major impact on the inflammatory responses of the vascular endothelium.

As shown by the changes in mRNA and protein levels of CCL2, we did observe that 10% surfactant in saline may influence the cytotoxicity potential of the MWCNT suspensions. Considering that under normal physiological conditions, surfactant is not encountered by endothelial cells and therefore could potentially initiate an inflammatory response in the endothelial cells upon contact. However, the presence of MWCNTs along with surfactant further aggravates the inflammatory response as evidenced by the up regulation of mRNA levels of cell adhesion molecules. To identify the net effect incurred by the MWCNTs and to eliminate the potential effect of the vehicle control to our data, we have normalized each MWCNT treated HAEC findings to the respective vehicle control.

VCAM1, SELE and *CCL2* were expressed relatively high at the mRNA level in the HAEC treated with (S)-MWCNTs. While CCL2 protein levels correlated with mRNA expression patterns, the same was not true for VCAM1 or SELE which were only slightly increased with MWCNT exposure. SELE and VCAM1 are cell adhesion molecules expressed on endothelial cells and mediate adhesion of leukocytes to vascular endothelium (Bevilacqua et al., 1989; Pelletier et al., 1992). The expression of VCAM1, ICAM1 and SELE were reported to be increased in endothelial cells following exposure to alumina nanoparticles (Oesterling et al., 2008) and SWCNTs (Zhiqing et al., 2010). SWCNT induced nuclear NF-κB/P65 translocation was reported to be inhibited by N-acetylcysteine, indicating elevated ICAM1 and VCAM1 expression is mediated by oxidative stress (Zhiqing et al., 2010). Changes in the mRNA levels in *VCAM1, ICAM1, IL8* and *CCL2* in human cardiac microvascular endothelial cells following exposure to several metal nanoparticles have also been reported (Sun et al., 2011). CCL2 (MCP1) is member of C-C chemokine family which recruits monocytes, memory T cells, and dendritic cells to sites of tissue injury, infection, and inflammation (Carr et al., 1994; Deshmane et al., 2009; Xu et al., 1996). CCL2 is also associated with the regulation of angiogenesis (Stamatovic et al., 2006), increased cytokine production (Semple et al., 2010) and systemic inflammatory responses (Tsuda et al., 2004). Up-regulation of these adhesion proteins and chemokine indicates the beginning of an array of intracellular and intercellular processes leading to inflammation. In addition to being endothelial markers, cell adhesion molecules will also determine the effects on the adjacent elements such as adherent leukocytes and vascular smooth muscle cells following MWCNT exposure which should be further studied using *in vitro* co-culture models or *in vivo* studies. In the absence of post transcriptional regulation the up-regulation of CCL2, VCAM 1 and SELE will lead to the chemo-attraction of monocytes and neutrophils to the site of endothelial injury/activation followed by macrophage activation and inflammation. The discrepancy between the mRNA and the protein levels of these chemokines and inflammatory markers in our study indicates that there are likely other pathways that are activated and regulate the translation of mRNA to protein, which is also supported by our pathway analysis data (Figure 6 C and D).

From our proteomics data and the pathway analysis, it was evident that following 24 h treatment with MWCNTs, each dose and type of suspension activates specific pathways in HAEC. The net outcome of these combinations of pathway activation and suppression will determine how the HAEC will respond MWCNT exposure. Interestingly, our data did not demonstrate a dose dependent increase in a majority of the proteins. Nevertheless, the magnitude of the fold change in the activated proteins in general was relatively higher with (S)-MWCNT. These observations suggest that the medium of suspension is important in determining the toxicity of the nanomaterials. This is further supported by previous studies on nanomaterials which have identified specific type, size, shape and dose differences in toxicity (Chaudhuri et al., 2010; Yang et al., 2009). Most studies have reported specific gene and protein changes but have not done a pathway analysis in detail. In our study, the eIF2 signaling pathway was identified by pathway analysis in both doses and suspensions of MWCNTs. This pathway involves eIF2 kinases that are activated in response to environmental stress to alleviate cellular injury or alternatively to induce apoptosis. The activation of different eIF2 kinases and subunits are responsible for both activating and deactivating the global protein translation in response to stress (Wek et al., 2006). The suppression of global protein translation by this pathway could provide an explanation for the discrepancy between the mRNA and protein levels observed in our study. This is further supported by the up-regulation of RNA post transcriptional modification seen with both types of MWCNT suspensions (Figure 6 C and D). To our knowledge, this is the first attempt where a detailed proteomics and pathway analysis has been done on the effects of MWCNT on human endothelial cells.

Another interesting finding in our study was the lack of cytotoxicity in HAEC following MWCNT exposure. When compared with the previous studies, we did not find significant changes in cell viability or large fold changes in IL8 mRNA (Walker et al., 2009) expression with either of the MWCNT suspensions in our study. Most of the cytotoxic changes seen in the other studies were significant but moderate in amplitude (Patlolla et al., 2010; Yang et al., 2009). This variability is most likely attributed to the dissimilarities in the type, dose, manufacturer, batch and contaminants of MWCNTs used in different studies. According to our characterization, the MWCNTs used in our study had relatively low contamination with metals and we adhered to all possible laboratory measures to prevent contamination with endotoxin and oxidative changes during storage and handling. Though the pure graphene sheets that are the fundamental building units of MWCNTs are considered relatively inactive, residual materials (Donaldson et al., 2006) and adjuvant compounds that bind to them in the suspension media could be the cause of underlying toxicity. Considering the *in vitro* approach, the source, type and passage of endothelial cells and components of the cell culture medium can also influence the level of cytotoxicity. Our conclusion is further supported by the findings of a recent study based on human umbilical vein endothelial cells, which reported reduced cytotoxicity of SWCNTs when they are bound to blood proteins (Ge et al., 2011). Lastly, the dosimetry of the MWCNTs used *in vitro* will greatly effect cytotoxicity and cell activation (Hinderliter et al., 2010). Our doses were based on mass since we were using the same material, but with different suspensions. However, since we observed a significant difference in stability of the MWCNT suspensions it is likely that surface area may change with time and therefore influence the responses we observed. The doses we used for the treatment of HAEC can be considered as relatively high for an inhalational exposure. However, they can also be considered as low and high doses (1 and 10 $\mu g/cm^2$) for an intravenous delivery depending on the blood concentration expected to be achieved in diagnostic or therapeutic applications. A recent assessment in a research laboratory producing MWCNTs found total-particulate concentrations ranging from 37 $\mu g/m^3$ – 430 $\mu g/m^3$ during airborne exposure to MWCNT in the absence of exposure controls (Han et al., 2008). The exact calculations on how these levels apply to endothelial cells remain to be determined based upon translocation and/or bio-distribution studies.

5. Conclusions

In conclusion, our data suggest that direct exposure to MWCNTs initiates a moderate inflammatory response in endothelial cells, which can be altered by changing the dose and suspension medium. Combining MWCNTs with other protein or lipid components that could vary depending on the properties of the biological system may also have an influence on this response. We also demonstrated that some protective, anti-oxidant and anti-inflammatory mechanisms are also being moderately expressed particularly at lower doses of (M)-MWCNTs. The relative low levels of up-regulation with (M)-MWCNTs suggest that dispersion medium will have a large influence on the use of MWCNTs as a mode of drug delivery. In contrast, inhalational exposure such as in an occupational setting may be more detrimental for the circulatory system if the MWCNTs consist of a pulmonary surfactant corona. Considering the current evidence on adverse cardiovascular outcomes of particulate matter (Allen et al., 2009; Cozzi et al., 2007; Rudra et al., 2011), it is essential that smaller novel nanomaterials undergo a toxicological assessment both *in vitro* and *in vivo* prior to their release for production and biomedical applications. *In vitro* systems have limited ability to detect these combined effects and further *in vivo* assessments are necessary to identify the specific changes before incorporating MWCNTs into biomedical applications.

Supplementary Material

Refer to Web version on PubMed Central for supplementary material.

Acknowledgments

This project was supported by grant numbers U19 ES019525 (JMB, TRF, CJW, SJS) and RC2 ES018025 (FAW) from the National Institute of Environmental Health Sciences. The content is solely the responsibility of the authors and does not necessarily represent the official views of the National Institute of Environmental Health Sciences or the National Institutes of Health.

We would like to thank Drs. Pu-Chun Ke and Apparao M. Rao for previous work on characterization of the dry powder form of the multiwalled carbon nanotubes. We also thank Dr. Walter Kline of ONY Inc. for the generous gift of Infasurf surfactant; Drs. Benjamin Harrison and Richard Czerw of Nanotech Labs Inc. for providing the multiwalled carbon nanotubes for this study.

Abbreviations

(S)-MWCNTs	multi-walled carbon nanotubes dispersed in 10% surfactant
(M)-MWCNTs	multi-walled carbon nanotubes dispersed in cell culture medium

References

Aiso S, Kubota H, Umeda Y, Kasai T, Takaya M, Yamazaki K, Nagano K, Sakai T, Koda S, Fukushima S. Translocation of intratracheally instilled multiwall carbon nanotubes to lung-associated lymph nodes in rats. Ind Health. 2011; 49:215–220. [PubMed: 21173528]

Allen RW, Criqui MH, Diez Roux AV, Allison M, Shea S, Detrano R, Sheppard L, Wong ND, Stukovsky KH, Kaufman JD. Fine particulate matter air pollution, proximity to traffic, and aortic atherosclerosis. Epidemiology. 2009; 20:254–264. [PubMed: 19129730]

Barrett EPJ, LG, Halenda PP. The determination of pore volume and area distributions in porous substances. I Computations from nitrogen isotherms. J Am Chem Soc. 1951; 73:373–380.

Bevilacqua MP, Stengelin S, Gimbrone MA Jr, Seed B. Endothelial leukocyte adhesion molecule 1: an inducible receptor for neutrophils related to complement regulatory proteins and lectins. Science. 1989; 243:1160–1165. [PubMed: 2466335]

Bianco A, Kostarelos K, Partidos CD, Prato M. Biomedical applications of functionalised carbon nanotubes. Chem Commun (Camb). 2005:571–577. [PubMed: 15672140]

Brunauer SE, PH, Teller E. Adsorption of Gases in Multimolecular Layers. J Am Chem Soc. 1938:309–319.

Carr MW, Roth SJ, Luther E, Rose SS, Springer TA. Monocyte chemoattractant protein 1 acts as a T-lymphocyte chemoattractant. Proc Natl Acad Sci U S A. 1994; 91:3652–3656. [PubMed: 8170963]

Chaudhuri P, Harfouche R, Soni S, Hentschel DM, Sengupta S. Shape effect of carbon nanovectors on angiogenesis. ACS Nano. 2010; 4:574–582. [PubMed: 20043662]

Cozzi E, Wingard CJ, Cascio WE, Devlin RB, Miles JJ, Bofferding AR, Lust RM, Van Scott MR, Henriksen RA. Effect of ambient particulate matter exposure on hemostasis. Transl Res. 2007; 149:324–332. [PubMed: 17543851]

Dai H. Carbon nanotubes: synthesis, integration, and properties. Acc Chem Res. 2002; 35:1035–1044. [PubMed: 12484791]

Deshmane SL, Kremlev S, Amini S, Sawaya BE. Monocyte chemoattractant protein-1 (MCP-1): an overview. J Interferon Cytokine Res. 2009; 29:313–326. [PubMed: 19441883]

Donaldson K, Aitken R, Tran L, Stone V, Duffin R, Forrest G, Alexander A. Carbon nanotubes: a review of their properties in relation to pulmonary toxicology and workplace safety. Toxicol Sci. 2006; 92:5–22. [PubMed: 16484287]

Gasser M, Rothen-Rutishauser B, Krug HF, Gehr P, Nelle M, Yan B, Wick P. The adsorption of biomolecules to multi-walled carbon nanotubes is influenced by both pulmonary surfactant lipids and surface chemistry. J Nanobiotechnology. 2010; 8:31. [PubMed: 21159192]

Ge C, Du J, Zhao L, Wang L, Liu Y, Li D, Yang Y, Zhou R, Zhao Y, Chai Z, Chen C. Binding of blood proteins to carbon nanotubes reduces cytotoxicity. Proc Natl Acad Sci U S A. 2011; 108:16968–16973. [PubMed: 21969544]

Han JH, Lee EJ, Lee JH, So KP, Lee YH, Bae GN, Lee SB, Ji JH, Cho MH, Yu IJ. Monitoring multiwalled carbon nanotube exposure in carbon nanotube research facility. Inhal Toxicol. 2008; 20:741–749. [PubMed: 18569096]

Hinderliter PM, Minard KR, Orr G, Chrisler WB, Thrall BD, Pounds JG, Teeguarden JG. ISDD: A computational model of particle sedimentation, diffusion and target cell dosimetry for in vitro toxicity studies. Part Fibre Toxicol. 2010; 7:36. [PubMed: 21118529]

Kim JE, Lim HT, Minai-Tehrani A, Kwon JT, Shin JY, Woo CG, Choi M, Baek J, Jeong DH, Ha YC, Chae CH, Song KS, Ahn KH, Lee JH, Sung HJ, Yu IJ, Beck GR Jr, Cho MH. Toxicity and clearance of intratracheally administered multiwalled carbon nanotubes from murine lung. J Toxicol Environ Health A. 2010; 73:1530–1543. [PubMed: 20954079]

Lacerda L, Ali-Boucetta H, Herrero MA, Pastorin G, Bianco A, Prato M, Kostarelos K. Tissue histology and physiology following intravenous administration of different types of functionalized multiwalled carbon nanotubes. Nanomedicine (Lond). 2008; 3:149–161. [PubMed: 18373422]

Lai X, Bacallao RL, Blazer-Yost BL, Hong D, Mason SB, Witzmann FA. Characterization of the renal cyst fluid proteome in autosomal dominant polycystic kidney disease (ADPKD) patients. Proteomics Clin Appl. 2008; 2:1140–1152. [PubMed: 20411046]

Lai X, Wang L, Tang H, Witzmann FA. A novel alignment method and multiple filters for exclusion of unqualified peptides to enhance label-free quantification using peptide intensity in LC-MS/MS. J Proteome Res. 2011; 10:4799–4812. [PubMed: 21888428]

Li J, Yang F, Guo G, Yang D, Long J, DF. Preparation of biocompatible multi-walled carbon nanotubes as potential tracers for sentinel lymph nodes. Polym Int. 2010; 59:169–174.

Li Z, Hulderman T, Salmen R, Chapman R, Leonard SS, Young SH, Shvedova A, Luster MI, Simeonova PP. Cardiovascular effects of pulmonary exposure to single-wall carbon nanotubes. Environ Health Perspect. 2007; 115:377–382. [PubMed: 17431486]

Lundqvist M, Stigler J, Cedervall T, Berggard T, Flanagan MB, Lynch I, Elia G, Dawson K. The evolution of the protein corona around nanoparticles: a test study. ACS Nano. 2011; 5:7503–7509. [PubMed: 21861491]

Oesterling E, Chopra N, Gavalas V, Arzuaga X, Lim EJ, Sultana R, Butterfield DA, Bachas L, Hennig B. Alumina nanoparticles induce expression of endothelial cell adhesion molecules. Toxicol Lett. 2008; 178:160–166. [PubMed: 18456438]

Patlolla A, Knighten B, Tchounwou P. Multi-walled carbon nanotubes induce cytotoxicity, genotoxicity and apoptosis in normal human dermal fibroblast cells. Ethn Dis. 2010; 20:S1-65–72. [PubMed: 20521388]

Pelletier RP, Ohye RG, Vanbuskirk A, Sedmak DD, Kincade P, Ferguson RM, Orosz CG. Importance of endothelial VCAM-1 for inflammatory leukocytic infiltration in vivo. J Immunol. 1992; 149:2473–2481. [PubMed: 1382105]

Rudra CB, Williams MA, Sheppard L, Koenig JQ, Schiff MA. Ambient carbon monoxide and fine particulate matter in relation to preeclampsia and preterm delivery in western Washington State. Environ Health Perspect. 2011; 119:886–892. [PubMed: 21262595]

Schmidt A, Goepfert C, Feitsma K, Buddecke E. Lovastatin-stimulated superinduction of E-selectin, ICAM-1 and VCAM-1 in TNF-alpha activated human vascular endothelial cells. Atherosclerosis. 2002; 164:57–64. [PubMed: 12119193]

Semple BD, Frugier T, Morganti-Kossmann MC. CCL2 modulates cytokine production in cultured mouse astrocytes. J Neuroinflammation. 2010; 7:67. [PubMed: 20942978]

Sinha R, Kim GJ, Nie S, Shin DM. Nanotechnology in cancer therapeutics: bioconjugated nanoparticles for drug delivery. Mol Cancer Ther. 2006; 5:1909–1917. [PubMed: 16928810]

Stamatovic SM, Keep RF, Mostarica-Stojkovic M, Andjelkovic AV. CCL2 regulates angiogenesis via activation of Ets-1 transcription factor. J Immunol. 2006; 177:2651–2661. [PubMed: 16888027]

Storey JD. A direct approach to false discovery rates. J Roy Stat Soc. 2002; B64:479–498.

Sun J, Wang S, Zhao D, Hun FH, Weng L, Liu H. Cytotoxicity, permeability, and inflammation of metal oxide nanoparticles in human cardiac microvascular endothelial cells: cytotoxicity, permeability, and inflammation of metal oxide nanoparticles. Cell Biol Toxicol. 2011; 27:333–342. [PubMed: 21681618]

Tsuda Y, Takahashi H, Kobayashi M, Hanafusa T, Herndon DN, Suzuki F. CCL2, a product of mice early after systemic inflammatory response syndrome (SIRS), induces alternatively activated macrophages capable of impairing antibacterial resistance of SIRS mice. J Leukoc Biol. 2004; 76:368–373. [PubMed: 15123772]

van der Zande M, Junker R, Walboomers XF, Jansen JA. Carbon nanotubes in animal models: a systematic review on toxic potential. Tissue Eng Part B Rev. 2011; 17:57–69. [PubMed: 21062222]

Walker VG, Li Z, Hulderman T, Schwegler-Berry D, Kashon ML, Simeonova PP. Potential in vitro effects of carbon nanotubes on human aortic endothelial cells. Toxicol Appl Pharmacol. 2009; 236:319–328. [PubMed: 19268679]

Wang X, Katwa P, Podila R, Chen P, Ke PC, Rao AM, Walters DM, Wingard CJ, Brown JM. Multi-walled carbon nanotube instillation impairs pulmonary function in C57BL/6 mice. Part Fibre Toxicol. 2011a; 8:24. [PubMed: 21851604]

Wang X, Xia T, Ntim SA, Ji Z, Lin S, Meng H, Chung CH, George S, Zhang H, Wang M, Li N, Yang Y, Castranova V, Mitra S, Bonner JC, Nel AE. Dispersal state of multiwalled carbon nanotubes elicits profibrogenic cellular responses that correlate with fibrogenesis biomarkers and fibrosis in the murine lung. ACS nano. 2011b; 5:9772–9787. [PubMed: 22047207]

Wek RC, Jiang HY, Anthony TG. Coping with stress: eIF2 kinases and translational control. Biochem Soc Trans. 2006; 34:7–11. [PubMed: 16246168]

Wenger Y, Schneider RJ 2nd, Reddy GR, Kopelman R, Jolliet O, Philbert MA. Tissue distribution and pharmacokinetics of stable polyacrylamide nanoparticles following intravenous injection in the rat. Toxicol Appl Pharmacol. 2011; 251:181–190. [PubMed: 21134391]

Xu LL, Warren MK, Rose WL, Gong W, Wang JM. Human recombinant monocyte chemotactic protein and other C-C chemokines bind and induce directional migration of dendritic cells in vitro. J Leukoc Biol. 1996; 60:365–371. [PubMed: 8830793]

Yang H, Liu C, Yang D, Zhang H, Xi Z. Comparative study of cytotoxicity, oxidative stress and genotoxicity induced by four typical nanomaterials: the role of particle size, shape and composition. J Appl Toxicol. 2009; 29:69–78. [PubMed: 18756589]

Zhiqing L, Zhuge X, Fuhuan C, Danfeng Y, Huashan Z, Bencheng L, Wei Z, Huanliang L, Xin S. ICAM-1 and VCAM-1 expression in rat aortic endothelial cells after single-walled carbon nanotube exposure. J Nanosci Nanotechnol. 2010; 10:8562–8574. [PubMed: 21121367]

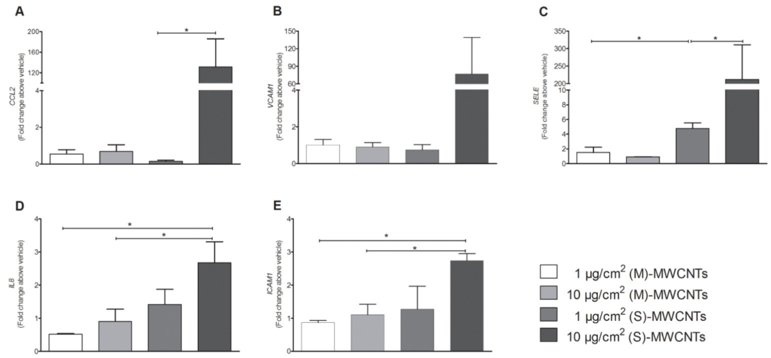

Figure 1.

Mean fold change in mRNA expression of cell adhesion molecules and chemokines in HAEC treated for 2 h with 1 μg/cm^2 and 10 μg/cm^2 of (M)-MWCNTs or (S)-MWCNTs. **A**. *CCL2*; **B**. *VCAM1*; **C.** *SELE*; **D**. *IL8*; **E**. *ICAM1*. The mean fold change represents the fold-change above vehicle treated HAEC and is based on 3–4 independent experiments.
** p<0.05,* when compared between the treatment groups, using a one tailed t test.

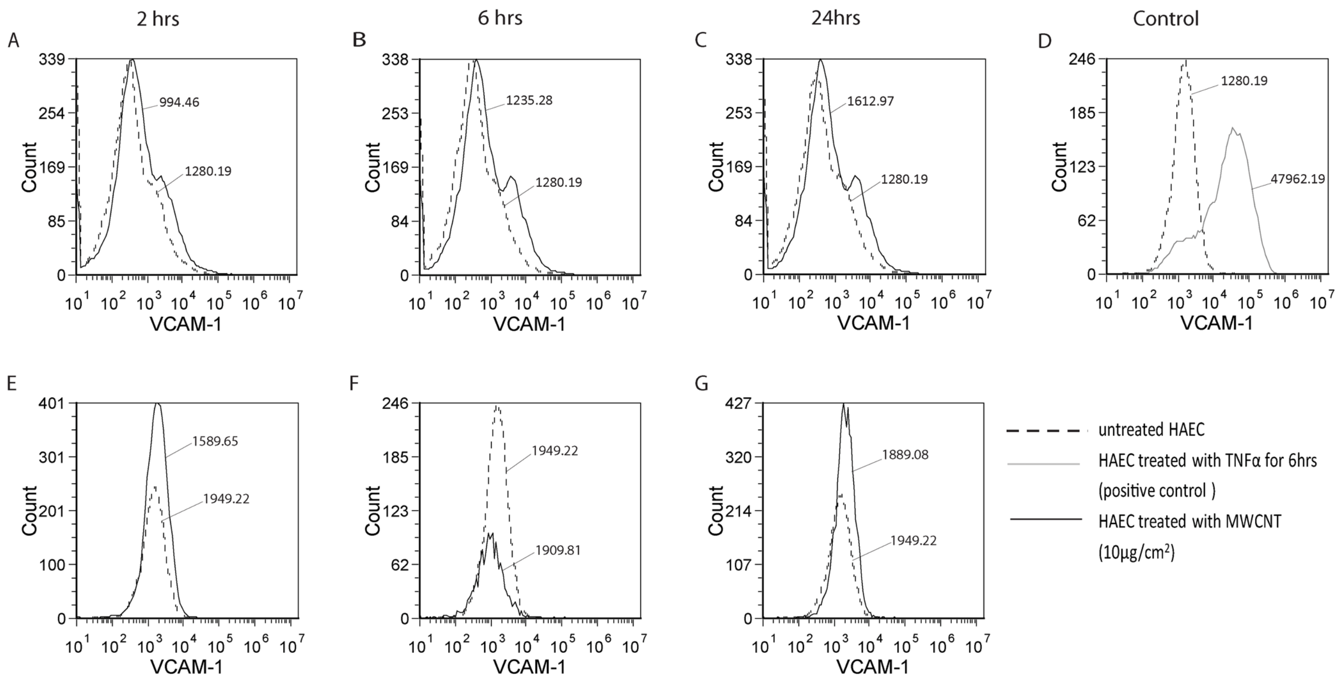

Figure 2.

Representative flow cytometery histograms for VCAM-1 following 2, 6 and 24 h of treatment with 10 μg/cm^2 MWCNTs. **A–C.** HAEC treated with (M)-MWCNTs; **D**. HAEC treated with 10 ng/ml of TNFα for 6 h (positive control); **E–G**. HAEC treated with (S)-MWCNTs. 10000 cell events were analyzed for each time point. Mean fluorescence intensity is represented by the numbers associated with each curve.

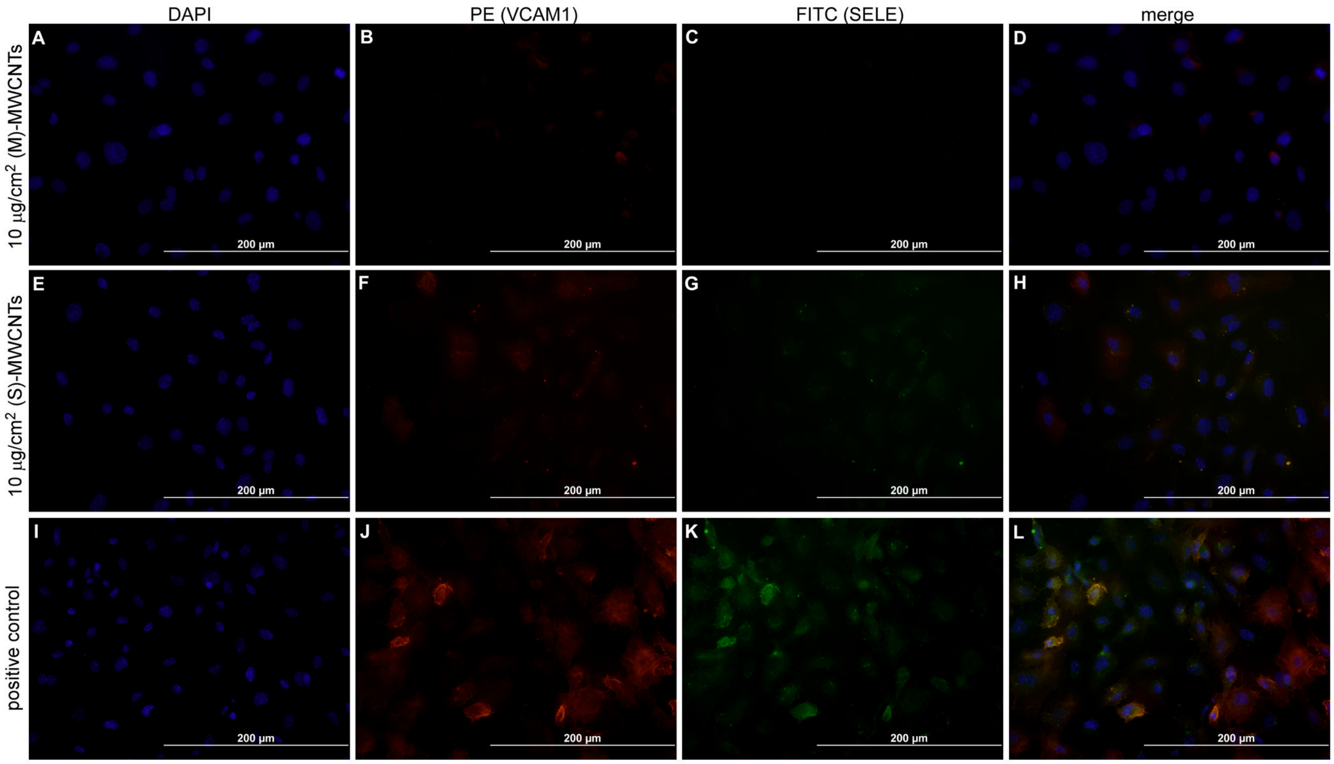

Figure 3.

Representative immunofluorescence images of HAEC stained for VCAM1 and SELE following treatment with 10 μg/cm^2 (M)-MWCNT **(A–D)**, 10 μg/cm^2 (S)-MWCNT **(E–H)** and TNFα (positive control; **I–L**) for 6 h. The nucleic acid stain DAPI (blue) localizes the nucleus. FITC (green) represents SELE staining and PE (red) represents VCAM1 staining which are mainly localized on the cell surface/cytoplasm. 40X magnification.

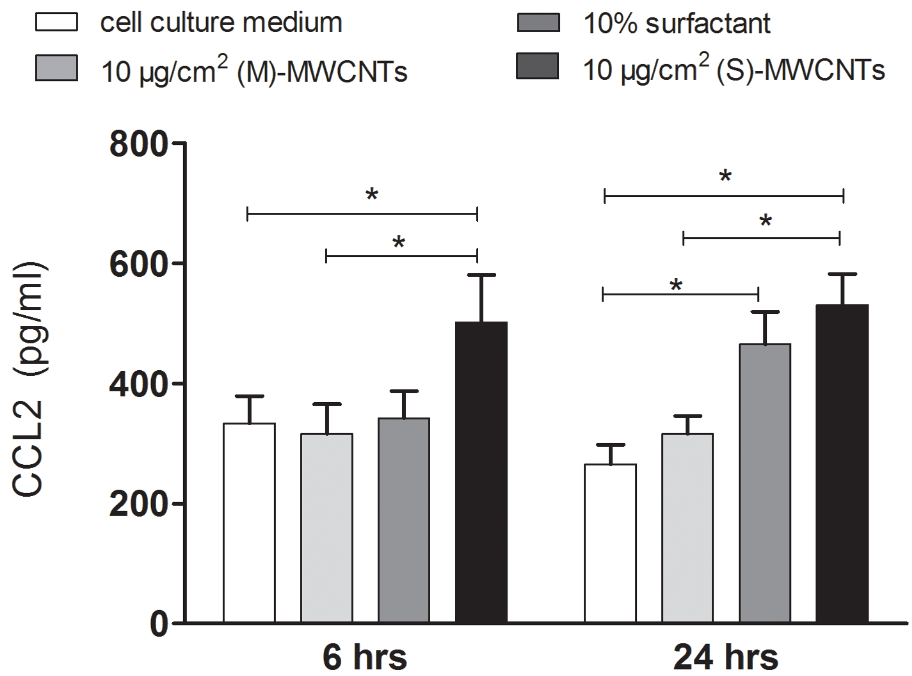

Figure 4.
CCL2 protein concentration measured by ELISA in the HAEC supernatant following treatment with 10 μg/cm^2 MWCNTs for 6 and 24 h. Each sample was analyzed in triplicate. The mean concentration of CCL2 represents data from 4–6 independent experiments. *$*p<0.05$.*

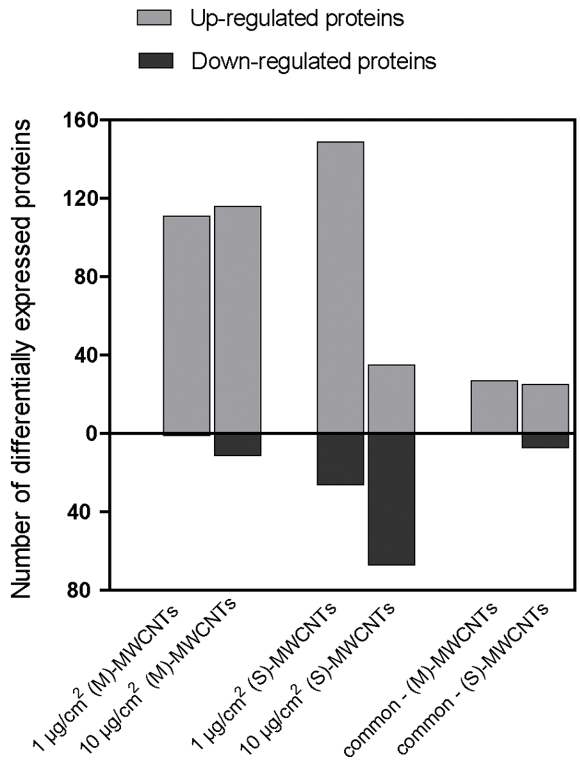

Figure 5.

Differential protein expression from 2,852 proteins analyzed following treatment with (M)-MWCNTs and 2,959 proteins analyzed following treatment with (S)-MWCNTs. The mean fold changes of 5 independent experiments were used for the analyses. The number of proteins with significant fold changes (p<0.05) when compared to medium or 10% surfactant are reported. Common = proteins with significant fold changes at both doses.

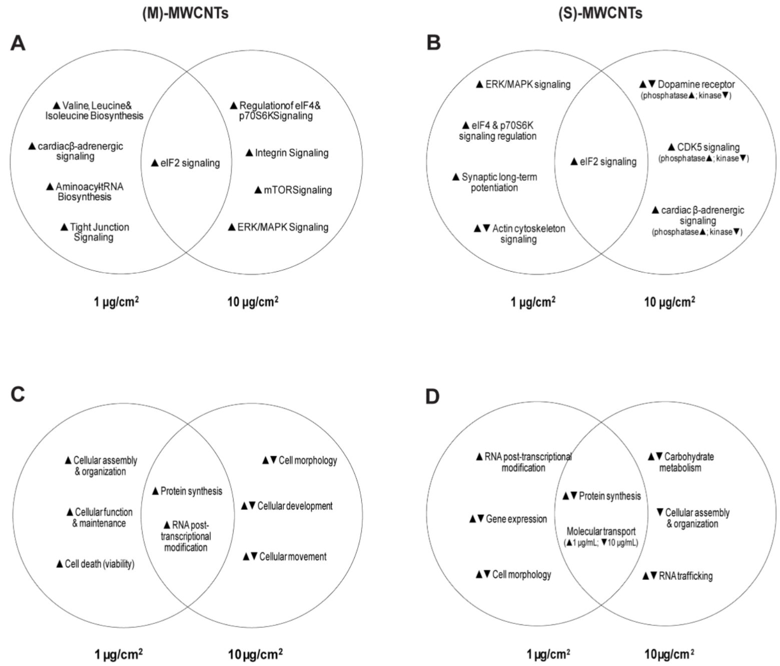

Figure 6.

Pathway analysis from differential protein expression studies. Canonical pathways altered by **A**. (M)-MWCNTs and **B**. (S)-MWCNTs. Cellular and molecular functions altered by **C**. (M)-MWCNTs and **D**. (S)-MWCNTs were identified based upon pathway analysis results. All the changes presented were statistically significant ($p<0.01$).

▲ = Up-regulation, ▼ = Down-regulation

Table 1

MWCNT characterization.

Characteristic	MWCNTs in dry powder form
Length	<2 μm
Mean diameter	Bimodal distribution with peaks at 12.5 nm and 25 nm
Surface area	113.10 m^2/g
Pore volume	0.68 cm^3/g
Raman spectra	Strong disorder band at 1350 cm^{-1}, $R=I_D/I_G = 0.65$
Elemental analysis	5% weight Fe catalyst

R = ratio, I_D = intensity of the disorder band (D-band), I_G = intensity of the graphite like band (G-band), Pore volume = MWCNT's air volume/ MWCNT's total volume

Table 2

Zeta potential and hydrodynamic size of different MWCNT suspensions

Zeta potential and hydrodynamic size was calculated using the means of three separate suspensions each consisting of 10 independent runs. The mean and the SEM are reported.

	(M)-MWCNTs	(S)-MWCNTs
Mean hydrodynamic size (nm)	970	915
Zeta potential (mV)	-15.3	-57.3

Table 3

Cell viability following MWCNT treatment of HAEC

Cell viability was determined using the MTS assay and the mean of 3 experiments are reported (% of cell viability). In addition, following 2, 6 and 24 h treatment of HAEC with MWCNT or vehicle, cells were stained with an ethidium homodimer to delineate dead cells and analyzed by flow-cytometry to calculate the percentage of dead cells. The mean of 3 experiments are reported. SD = standard deviation

Treatment	MTS Assay (% of cell viability ± SD)			Live/Dead Assay (% of dead cells ± SD)		
	2 h	6 h	24 h	2 h	6 h	24 h
cell culture medium only	95.8 ± 1.1	101.9 ± 2.8	102.2 ± 2.5	2.8 ± 0.6	3.3 ± 0.7	3.6 ± 1.8
1 mg/cm^2 (M)-MWCNTs	104.7 ± 12.4	98.4 ± 2.5	98.41 ± 1.4	3.8 ± 1.4	3.6 ± 0.8	1.9 ± 0.2
10 mg/cm^2 (M)-MWCNTs	110.8 ± 7.1	95.4 ± 4.0	87.71 ± 0.6	5.6 ± 1.0	4.6 ± 1.0	3.5 ± 0.8
10% surfactant in saline	96.1 ± 9.1	92.8 ± 3.2	108.9 ± 1.9	1.6 ± 0.4	1.4 ± 0.3	4.2 ± 0.4
1 mg/cm^2 (S)-MWCNTs	101.1 ± 4.4	92.1 ± 1.4	108.9 ± 0.8	2.8 ± 0.9	2.6 ± 0.3	2.8 ± 0.5
10 mg/cm^2 (S)-MWCNTs	101.4 ± 3.7	97.2 ± 3.7	112.9 ± 2.3	4.6 ± 0.8	4.6 ± 0.3	4.5 ± 0.8